LCC-HVDC Small Signal Model Considering the Influence of Voltage Variation

Zhiyu Li, Chongru Liu, Juehao Xie
State Key Laboratory of Alternate Electrical Power System with Renewable Energy Sources
North China Electric Power University
Beijing, China
lizhiyu_ncepu@163.com

Huan Li, Wei Wei
Electric Power Research Institute
China Southern Power Grid
Guangzhou, Guangdong, China

2021 IEEE 4th International Electrical and Energy Conference (CIEEC) | 978-1-7281-7149-4/21/$31.00 ©2021 IEEE | DOI: 10.1109/CIEEC50170.2021.9511040

***Abstract*—The High Voltage Direct Current (HVDC) technology is developing rapidly in China due to long distance power transfer, large power handling capacity and low loss. In this paper, a small signal model considering the influence of voltage variation is proposed for fast and accurate simulation of AC/DC hybrid power grid. First, the LCC-HVDC state space model is developed where voltage and power are selected as the converter station interface to make the model generation easier. Later, the influence of dynamic voltage variation on the converter station model during the small disturbance is considered. The quasi-steady state model and the commutation angle formula were revised to improve the accuracy of the small signal model. The correctness of the small signal model of the HVDC transmission system established in this paper is verified.**

Keywords—HVDC transmission; small signal model; commutation angle calculation; converter station model

I. INTRODUCTION

The Line Commutated Converter based High Voltage Direct Current (LCC-HVDC) is an effective technology to solve the problem of long distance power transfer and large power transmission [1-2]. The small signal stability analysis has been widely used in LCC-HVDC controller parameter selection and damping analysis. The accurate model for LCC-HVDC small signal directly influences the stability analysis. Therefore, a research on small signal model is given in this paper.

The small signal model of the LCC-HVDC system is mostly obtained by linearizing the quasi-steady state model [3]. In [4-5], a quasi-steady state model of DC transmission line including LCC converter station and control system is established. In [6-7], a time-domain linearization model of UHVDC based on the quasi-steady state model of LCC converter station is established. In [8-9], the time-domain model is transformed to frequency-domain model, and a small signal modeling method of LCC-HVDC considering harmonic coupling is proposed. In [10-13], the system is divided into several subsystems based on the idea of modular modeling, which greatly reduces the complexity of unified modeling and also provides the possibility to analyze the dynamic interaction process between subsystems. In [14], a small signal model of LCC-HVDC from the perspective of output current vector and DC current is proposed to describe its external characteristics.

However, the models in literature either have insufficient accuracy or too complex to be used in system analysis. Moreover, the existing small signal models of converter station mostly select the voltage and current on both sides of AC and DC system to establish the relationship. This form of models use current and voltage relationships in the *xy* coordinate, which leads to the complex process of model establishment, large amount of calculations and difficulty of computer programming.

Aiming at the above mentioned problems of insufficient model accuracy and complex model interface, a LCC-HVDC small signal model with simple modeling and high accuracy is proposed in this paper. The model has two characteristics: (1) Voltage and power are used as the interface variable of converter station to establish the connection between AC and DC system which makes the model easier to establish; (2) A differential equation that takes into account the influence of the voltage on the trigger angle is added to the model, since the voltage variation on the AC side of the converter station will affect the trigger angle when there is small disturbance, which improves the accuracy of the quasi-steady state model. The correctness of the proposed model and the validity of improving the accuracy of the model are verified by comparing with the results of PSCAD electromagnetic transient simulations.

II. THE INFLUENCE OF VOLTAGE VARIATION ON SMALL SIGNAL MODEL

Existing models generally believe that the commutation angle formula is:

$$\cos\gamma = \cos\beta_i + \frac{\sqrt{2}X_{ci}I_{di}}{k_i E_{aci}} = -\cos\alpha_i + \frac{\sqrt{2}X_{ci}I_{di}}{k_i E_{aci}} \qquad (1)$$

Where γ is the extinction angle of the inverter. The α_i is the actual trigger angle of the inverter. The β_i is the trigger lead angle of the inverter.

During steady-state operation, the grid-side voltage of the converter station does not change. Take the voltage operating in E_1 as an example (as shown in Fig. 1), the period between points A and B is half cycle and the phase angle is π. It means

This work was supported by science and technology project of China Southern Power Grid (ZBKJXM20180104).

978-1-7281-7149-4/21/$31.00 ©2021 IEEE

the angle between the two natural commutation points of the line voltage is π i.e. $\alpha+\beta=\pi$.

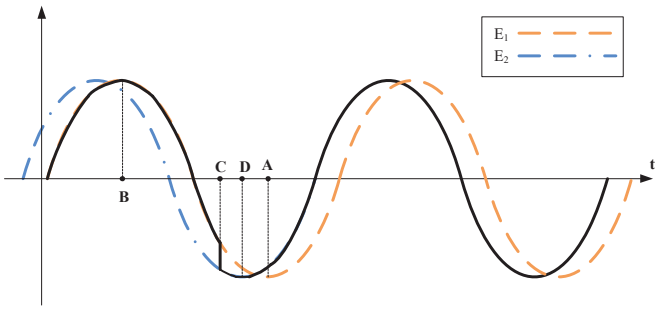

Fig. 1. Schematic diagram of voltage variation.

Here, when the system voltage changes from E_1 to E_2 due to small disturbance at time C, the half cycle of voltage is represented between two points B and D. It can be seen from the figure that the angle between two natural commutation points of line voltage is not equal to π, and the (1) is no longer strictly true.

Considering the influence of voltage variation on small signal model, define the difference between the angle between two natural commutation points of the same line voltage and π as θ_π:

$$\theta_\pi=\theta_{ac}-\theta_{ac}e^{-sT/2} \tag{2}$$

Where θ_{ac} is the grid side bus voltage angle of the converter. The T is the voltage period for a 50Hz system i.e. $T=0.02s$. The θ_π is 0 in the steady state and satisfies $\alpha+\beta+\theta_\pi=\pi$ when the voltage changes.

Parder approximation for the delay in (2).

$$\theta_\pi=\theta_{ac}-\theta_{ac}\frac{1-sT/4}{1+sT/4}=\frac{sT/2}{1+sT/4}\theta_{ac} \tag{3}$$

Substitute $\theta_{\pi 2}=\theta_{ac}-\theta_\pi/2$ in (3).

$$\theta_{\pi 2}=\frac{1}{1+sT/4}\theta_{ac} \tag{4}$$

According to (4), a new state equation can be obtained where $T_\pi=T/4=0.005s$.

$$T_\pi\dot{\theta}_{\pi 2}=\theta_{ac}-\theta_{\pi 2} \tag{5}$$

The extinction angle γ of the inverter after considering the influence of the voltage variation would become as (6).

$$\gamma=\arccos(\cos(\pi-\theta_\pi-\alpha)+\frac{\sqrt{2}X_{ci}I_{di}}{k_iE_{aci}}) \tag{6}$$

III. Small Signal Model Considering the Influence of Voltage Variation

A. System Structure

In this paper, a 12-pulse LCC HVDC is used to carry out the research. The block diagram of system under study is shown in Fig. 2. Here, the subscript "*r*" represents the rectifier and "*i*" represents the inverter. The $\boldsymbol{E_{ac}}$ is the effective value of the converter bus voltage and k is the conversion ratio of the converter transformer. The $\boldsymbol{X_c}$ is the equivalent commutation reactance of the converter transformer. The DC transmission line is modeled as equivalent T-configuration. The L and R represent the equivalent reactance and resistance of the DC line, respectively. The C denotes the equivalent capacitance of the DC line to ground and $\boldsymbol{I_d}$ is the DC current. The positive direction is shown by the arrow in Fig. 2.

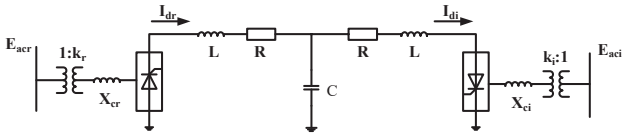

Fig. 2. LCC-HVDC transmission system structure.

B. Quasi-steady State Model of DC system

1) DC transmission line

In Fig. 2, the DC line is modelled as lumped parameter. According to Kirchhoff's voltage law, the quasi-steady state model of the DC line can be formulated as:

$$\begin{cases} L\dot{I}_{dr}=V_{dr}-V_c-RI_{dr} \\ L\dot{I}_{di}=V_c-V_{di}-RI_{di} \\ C\dot{V}_d=I_{dr}-I_{di} \end{cases} \tag{7}$$

Where V_{dr}, V_{di} are DC voltage at rectifier and inverter side, respectively. The V_c is voltage across capacitance of DC line.

2) Converter station

The quasi-steady state model mainly considers the fundamental wave components. Each quantity in the equation is the average value of power frequency. The equation on the rectifier side is [15]:

$$\begin{cases} V_{dr}=\dfrac{3\sqrt{2}}{\pi}nk_rE_{acr}\cos\alpha_r-\dfrac{3}{\pi}nX_{cr}I_{dr} \\ P_{dr}=V_{dr}I_{dr} \\ Q_{dr}=I_{dr}\sqrt{\left(\dfrac{3\sqrt{2}}{\pi}nk_rE_{acr}\right)^2-V_{dr}^{\ 2}} \\ \alpha_r=\alpha_r'+\theta_{acr}-\theta_{PLLr} \end{cases} \tag{8}$$

Where n is the number of bridges in series of converter. The α_r is the actual trigger angle of rectifier. The P_{dr} *and* Q_{dr} are the rectifier side active and reactive power injected into the converter station from the AC grid. The α_r' is the trigger angle instruction value output by the rectifier side controller. The θ_{acr} is the grid side bus voltage angle of the converter. The θ_{PLLr} is the rectifier side phase locked loop output angle.

The mathematical model of the inverter station after considering the influence of voltage variation on the small signal model would become as (9):

$$\begin{cases} T_\pi \dot{\theta}_{\pi 2} = \theta_{ac} - \theta_{\pi 2} \\ V_{di} = \dfrac{3\sqrt{2}}{\pi} n k_i E_{aci} \cos\gamma - \dfrac{3}{\pi} n X_{ci} I_{di} \\ \alpha_i + \beta_i + \theta_\pi = \pi \\ \cos\gamma = \cos\left(\pi - \theta_\pi - \alpha\right) + \dfrac{\sqrt{2} X_{ci} I_{di}}{k_i E_{aci}} \\ P_{di} = V_{di} I_{di} \\ Q_{di} = -I_{di} \sqrt{\left(\dfrac{3\sqrt{2}}{\pi} n k_i E_{aci}\right)^2 - V_{di}^2} \\ \alpha_i = \alpha_i' + \theta_{aci} - \theta_{PLLi} \\ \theta_{\pi 2} = \theta_{ac} - \dfrac{\theta_\pi}{2} \end{cases} \tag{9}$$

Where γ is the extinction angle of the inverter. The α_i is the actual trigger angle of the inverter. The β_i is the trigger lead angle of the inverter. The P_{di} *and* Q_{di} are the inverter side active and reactive power injected into the converter station from the AC grid. The α_i' is the trigger angle instruction value output by the inverter side controller. The θ_{aci} is the grid side bus voltage angle. The θ_{PLLi} is the inverter side phase locked loop output angle.

3) DC control system

The DC control system of LCC-HVDC is mainly composed of a trigger angle controller and phase locked loop controller. The trigger angle controller is mainly composed of first-order inertia link and PI controller. In this paper, the quasi-steady state model of DC control system is established by taking the rectifier side as constant current control and the inverter side as constant extinction angle control.

The rectifier station adopts constant current control, and its controller structure is shown in Fig. 3.

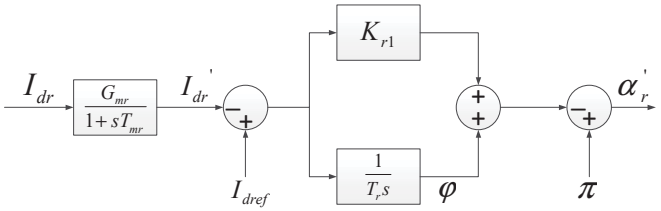

Fig. 3. Constant current control structure diagram.

The corresponding quasi-steady state model can be written as (10).

$$\begin{cases} T_{mr} \dot{I}_{dr}' = G_{mr} I_{dr} - I_{dr}' \\ \dot{\phi} = \dfrac{1}{T_r}\left(I_{dref} - I_{dr}'\right) \\ \alpha_r' = \pi - \phi - K_{r1}\left(I_{dref} - I_{dr}'\right) \end{cases} \tag{10}$$

Where I_{dr} is the rectifier side DC line current. The I_{dr}' is the DC current filtered by the first order inertia link. The T_{mr} and G_{mr} are the time constant and gain coefficient of the first order system. The I_{ref} is the reference value of the constant current controller. The φ is the output of the integral link in the PI controller. The T_r and K_{r1} are the integral time constant and proportional gain of the PI controller. The α_r' is the trigger angle instruction value output by the controller.

The inverter station adopts constant extinction angle control, and its controller structure is shown in Fig. 4.

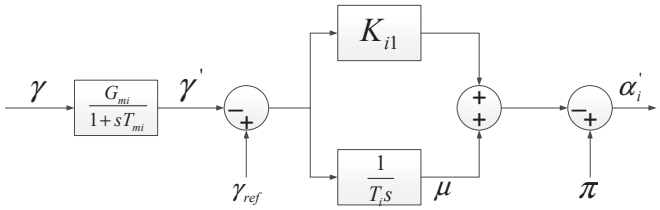

Fig. 4. Constant extinction angle control structure diagram.

The corresponding quasi-steady state model can be written as (11).

$$\begin{cases} T_{mi} \dot{\gamma}' = G_{mi} \gamma - \gamma' \\ \dot{\mu} = \dfrac{1}{T_i}\left(\gamma_{ref} - \gamma'\right) \\ \alpha_i' = \pi - \mu - K_{i1}\left(\gamma_{dref} - \gamma'\right) \end{cases} \tag{11}$$

Where γ is the extinction angle of the inverter. The γ' is the extinction angle filtered by the first order inertia link. The T_{mi} and G_{mi} are the time constant and gain coefficient of the first order control system. The γ_{ref} is the reference value of the constant current controller. Generally, the γ_{ref} is 0.2618. The μ is the output of the integral link in the PI controller. The T_i and K_{i1} are the integral time constant and proportional gain of the PI controller. The α_i' is the trigger angle instruction value output by the controller.

The phase locked loop (PLL) generates the correction of the trigger angle of the converter station through a negative feedback signal by measuring the change of the voltage phase angle of the converter bus. The block diagram is shown in Fig. 5.

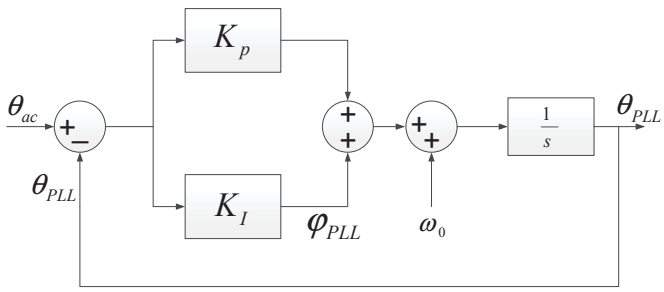

Fig. 5. PLL structure diagram.

The corresponding quasi-steady state model can be written as (12).

$$\begin{cases} \dot{\phi}_{PLLr(i)} = K_{Ir(i)}\left(\theta_{acr(i)} - \theta_{PLLr(i)}\right) \\ \dot{\theta}_{PLLr(i)} = \phi_{PLLr(i)} + K_{pr(i)}\left(\theta_{acr(i)} - \theta_{PLLr(i)}\right) \end{cases} \tag{12}$$

Where the subscripts r and i represent the rectifier and the inverter side, respectively. The φ_{PLL} is the output of the integration link in the PI controller of PLL. The θ_{ac} is the grid side bus voltage angle of the converter. The ω_0 is the bus voltage angular frequency at the network side of the converter transformer. The K_p and K_i are proportional and integral gain of PI controller. The θ_{PLL} is the output angle of PLL.

C. Selection of DC System Interface Variables

In this research work, voltage and power are used as the interface variable for the converter station to establish the connection between AC and DC systems. The mathematical equation of the proposed algorithm for the small signal model of AC-DC network is written as (13).

$$\begin{bmatrix} \Delta \boldsymbol{P} \\ \Delta \boldsymbol{Q} \end{bmatrix} = \boldsymbol{Z} \begin{bmatrix} \Delta \boldsymbol{E}_{ac} \\ \Delta \boldsymbol{\theta}_{ac} \end{bmatrix} \tag{13}$$

Where $\boldsymbol{P}$ and $\boldsymbol{Q}$ are the active and reactive power injected into the network node. The $\boldsymbol{E_{ac}}$ and $\boldsymbol{\theta_{ac}}$ are the amplitude and phase angle of the node voltage. The proposed method has the following advantages: (1) The quasi-steady state model of most components in the power system is expressed in the form of voltage phasor equations. The small-signal model can be obtained by directly linearizing the quasi-steady-state model, which is conducive to the combination of AC and DC system models. (2) For AC system, the $\boldsymbol{Z}$ in (13) represents the corresponding Jacobian matrix $\boldsymbol{J}$, which can directly be obtained by power flow calculation.

D. Small Signal Model Considering Voltage Variation

After considering the influence of voltage variation on the angle relationship and commutation angle. The state space model of LCC-HVDC system is composed of (7) ~ (12).

The simplified state space model of the proposed technique can be written as (14).

$$\begin{aligned} \dot{\boldsymbol{x}} &= f(\boldsymbol{x}, \boldsymbol{y}, \boldsymbol{u}) \\ \boldsymbol{p} &= g(\boldsymbol{x}, \boldsymbol{y}, \boldsymbol{u}) \end{aligned} \tag{14}$$

Where state variable $\boldsymbol{x}=[I_{dr}, I_{dr}', \varphi, \varphi_{PLLr}, \theta_{PLLr}, I_{di}, \gamma', \mu, \varphi_{PLLi}, \theta_{PLLi}, \theta_{\pi 2}, V_c]^T$; algebraic variable $\boldsymbol{y}=[E_{acr}, \theta_{acr}, E_{aci}, \theta_{aci}]^T$; input variable $\boldsymbol{u}=[I_{dref}, \gamma_{dref}]^T$; $\boldsymbol{p}=[P_{dr}, Q_{dr}, P_{di}, Q_{di}]^T$.

After linearization, the simplified equations become as (15).

$$\begin{cases} \Delta \dot{\boldsymbol{x}} = \boldsymbol{A}\Delta \boldsymbol{x} + \boldsymbol{B}\Delta \boldsymbol{y} + \boldsymbol{M}\Delta \boldsymbol{u} \\ \Delta \boldsymbol{p} = \boldsymbol{C}\Delta \boldsymbol{x} + \boldsymbol{D}\Delta \boldsymbol{y} + \boldsymbol{N}\Delta \boldsymbol{u} \end{cases} \tag{15}$$

Where $\boldsymbol{A}=\partial f/\partial x|_{x=x0}$, $\boldsymbol{B}=\partial f/\partial y|_{y=y0}$, $\boldsymbol{C}=\partial g/\partial x|_{x=x0}$, $\boldsymbol{D}=\partial g/\partial y|_{y=y0}$, $\boldsymbol{M}=\partial f/\partial u|_{u=u0}$, $\boldsymbol{N}=\partial g/\partial u|_{u=u0}$.

The power equation of AC side is as (16).

$$\Delta \boldsymbol{p} = \boldsymbol{J}\Delta \boldsymbol{y} \tag{16}$$

Small signal model of LCC-HVDC can be obtained by combining (15) and (16).

$$\Delta \dot{\boldsymbol{x}} = \left[\boldsymbol{A} - \boldsymbol{B}\left(\boldsymbol{D} - \boldsymbol{J}\right)^{-1} \boldsymbol{C} \right] \Delta \boldsymbol{x} + \left[\boldsymbol{M} - \boldsymbol{B}\left(\boldsymbol{D} - \boldsymbol{J}\right)^{-1} \boldsymbol{N} \right] \Delta \boldsymbol{u} \tag{17}$$

IV. Model Validation

In order to validate the correctness of the small signal model considering the influence of voltage variation, the electromagnetic transient model of the system is developed in PSCAD as shown in Fig. 1. At $t=10s$, the reference value I_{dref} of the constant current controller changes from 1.0 p.u. to 0.95 p.u. The electromagnetic transient simulation results are compared with the calculation results of the conventional small signal model (SSM) and the small signal model considering voltage variation (SSM-CVV) established in this paper. The results are shown in Fig. 6 to Fig. 9.

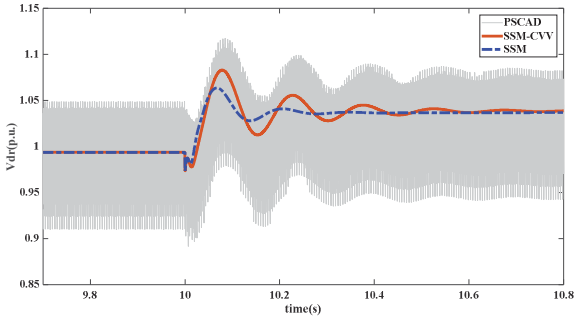

Fig. 6. Rectifier side DC voltage V_{dr}.

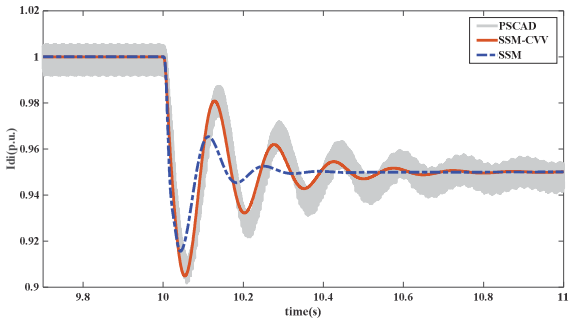

Fig. 7. Inverter side DC current I_{di}.

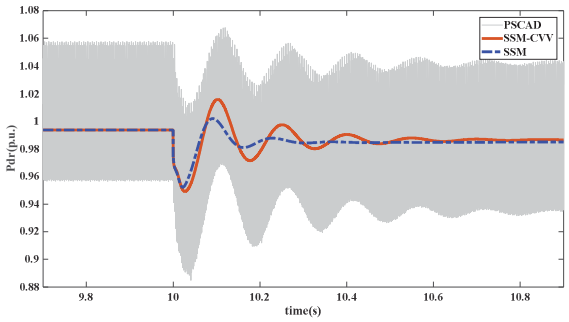

Fig. 8. Rectifier side active power P_{dr}.

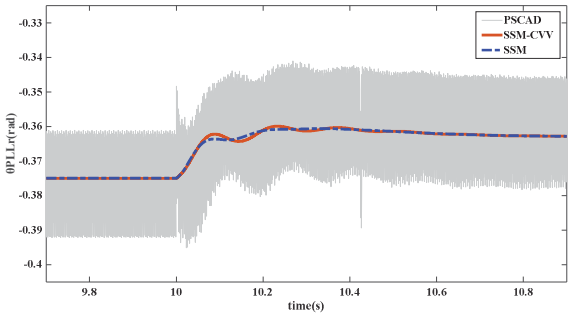

Fig. 9. PLL output phase θ_{PLLr}.

After comparing the conventional small signal model with the SSM-CVV results established in this paper, the characteristic values and oscillation frequencies of the system are shown in Table 1.

TABLE I. COMPARISON OF SYSTEM CHARACTERISTIC VALUE AND OSCILLATION FREQUENCY

SSM		SSM-CVV	
Characteristic value	***Frequency (Hz)***	***Characteristic value***	***Frequency (Hz)***
-1643.59+j0	-	-2362.61+j0	-
-665.41+j0	-	-692.91+j0	-
-103.78±j264.02	42.02	-430.50+j0	-
-188.76+j0	-	-146.18±j238.01	37.89
-13.80±j44.89	7.14	-77.34+j0	-
-4.75±j4.70	0.75	-6.48±j 42.12	6.70
-5.11±j5.10	0.81	-4.75±j 4.69	0.75
		-5.11±j5.10	0.81

Since PSCAD is an electromagnetic transient simulation, and the DC control system only filters low-order harmonics, there are some high-order harmonics in the waveform. Since the Prony analysis can analyze the accurate amplitude and frequency of the signal from the waveform, PSCAD is fitted by the Prony analysis method. The model error is analyzed with accurate frequency and model calculation frequency.

The Prony analysis results of PSCAD curves are shown in Table 2. Only the signal data with large amplitude and clear influence on the system are listed in Table 2. It can be seen from Table 2 that the dominant oscillation frequency in the transient process is 6.6 Hz.

TABLE II. PRONY ANALYSIS RESULTS

Mode	Amplitude	Frequency (Hz)
1 DC	1.9	-
2 Sine	0.048	6.6
3 DC	0.033	-
4 Sine	0.016	37
5 DC	0.01	-

It can be seen from Fig. 3 to Fig. 6 that the SSM model is not accurate enough to describe the transient processes. It leads to a larger error between the calculated dominant oscillation frequency of 7.14 Hz and the actual oscillation frequency of 6.6 Hz, and the relative error is 8.1%. Compared with the SSM model, the dimension of SSM-CVV model established in this paper is only increased by one order and its calculation results are consistent with the PSCAD electromagnetic transient simulation results. Hence, the SSM-CVV model accurately describes the transient oscillation process of the system. The calculation results of the dominant oscillation frequency of 6.7 Hz are closer to the actual oscillation frequency, and the relative error is 1.5%. The error may be due to the lack of consideration of the effect of oscillation on the thyristor commutation process. But by comparing with the SSM model, the proposed model has obviously higher accuracy.

V. CONCLUSION

In this paper, a small signal model considering the influence of voltage variation is proposed to solve the low accuracy and complexity issues of small signal model of DC system. Here, the voltage and power are used as the converter station interface variable to establish the connection between AC and DC systems. The formation of small signal model is easier compared to traditional current and voltage technique.

The influence of AC side voltage variation on the angle relationship and commutation angle of the converter station is considered. The accuracy of the model is improved by introducing new state and output equations. The proposed small signal model considering voltage variation can accurately simulate dynamic signal response as simulated in PSCAD electromagnetic transient program. The proposed method not only simplifies the model, but also improves the accuracy of small signal model with lower model order.

Acknowledgment

This work was supported by science and technology project of China Southern Power Grid (ZBKJXM20180104).

The authors gratefully acknowledge the contributions of Bilawal Rehman with National Skills University Islamabad, Pakistan to his great suggestion to this document.

References

[1] Y. Li, "Technology and Practice of the Operation Control of Large Power Grid Connected With Weak AC area," Power System Technology, vol.40, pp.3756-3760, 2016.

[2] G. Tang, Z. He and H. Pang, "Basic topology and key devices of the five-terminal DC grid," CSEE Journal of Power and Energy System, vol. 1, pp.22-35, 2015.

[3] Y. He, W. Xiang, J. Zhou, J. Zhao and J. Wen, "Small Signal Modelling of LCC-MMC Series Hybrid HVDC Transmission System," Transactions of China Electrotechnical Society, 2020.

[4] C. Guo, C. Zhao, R. Iravani, H. Ding and X. Wang, "Impact of phase-locked loop on small-signal dynamics of the line commutated converter-based high-voltage direct-current station," IET Generation, Transmission & Distribution, vol. 11, 2017.

[5] W. Chen, Y. Ye, B. Zhou, et al, "Influence of Constant Voltage Control and Predictive Constant Extinction Angle Control on Small-signal Stability of HVDC," Automation of Electric Power Systems, vol. 44, pp.98-111,2020.

[6] X. Wang, Q. Chen, Y. Zhang, et al, "Modal Analysis on System Stability of UHVDC Hierarchical Connection to AC Grid," Power System Technology, vol. 42, pp.2869-2878, 2018.

[7] C. Karawita, U. Annakkage, "Multi-infeed HVDC interaction studies using small-signal stability assessment," IEEE Transactions on Power Delivery, vol.24, pp.910-918, 2009.

[8] Y. Qi, H. Zhao, S. Fan, et al, "Small Signal Frequency-Domain Model of a LCC-HVDC Converter Based on an Infinite Series-Converter Approach," IEEE Transactions on Power Delivery, vol.34, 2019.

[9] P. Zhou, T. Liu, S. Wang, J. Ma, H. Zhang, "Small Signal Modeling of LCC-HVDC Station with Consideration of Harmonic Coupling Characteristics," Power System Technology, 2020.

[10] Z. Zhen, W. Du, H. Wang, "Small Signal Stability Analysis of Multi-Infeed HVDC System," Southern Power System Technology, vol.12, pp.29-36, 2018.

[11] C. Karawita, U. Annakkage, "Control block diagram representation of an HVDC system for sub-synchronous frequency interaction studies," Proceedings of the 9th IET International Conference on AC and DC Power Transmission. London: IET, 2011.

[12] Q. Fu, W. Du, H. Wang, "Small Signal Stability Analysis of AC/DC Hybrid Power System: An Overview ," Proceedings of the CSEE, vol.38, pp.2829-2840, 2018.

[13] C. Guo, Z. Yin, C. Zhao, R. Iravani, "Small-signal dynamics of hybrid LCC-VSC HVDC systems," International Journal of Electrical Power and Energy Systems, 2018.

[14] J. Lu, X. Yuan, J. Hu, et al. " Motion equation modeling of LCC-HVDC station for analyzing DC and AC network interactions," IEEE Transactions on Power Delivery, 2020.

[15] Y. He, X. Zheng, N. Tai, et al, "A Review of Modeling Methods for LCC-HVDC Converter in AC/DC Hybrid Power Grid," Proceedings of the CSEE, vol.39, pp.3119-3130, 2019.